

A General Polymer-Based Process To Prepare Mixed Metal Oxides: The Case of $\text{Zn}_{1-x}\text{Mg}_x\text{O}$ Nanoparticles

Guangqiang Lu, Ingo Lieberwirth, and Gerhard Wegner*

Contribution from the Max Planck Institute for Polymer Research, Ackermannweg 10, D-55128, Mainz, Germany

Received May 31, 2006; E-mail: wegner@mpip-mainz.mpg.de

Abstract: Nanometer-sized mixed metal oxide (MMO) particles ($\text{Zn}_{1-x}\text{Mg}_x\text{O}$) with very precise stoichiometry are prepared employing a polymer-based method. The precursor is formed by loading a polyacrylate with metal ions followed by purification of the polymer metal ion complex via repeated precipitation/redissolution cycles. Calcination of the polymer precursor at 550 °C gives particles of the metastable solid solution of the ZnO/MgO system in the composition range ($x < 0.2$ and $x \geq 0.82$). The MMO crystal particles are typically 20–50 nm in diameter. Doping of the ZnO by Mg^{2+} causes a shrinkage of lattice parameter c . Effects of band gap engineering on the optical band gap are reported. The photoluminescence in the visible is also affected, and its maximum shifts from 2.12 eV (pure ZnO) to 2.32 eV at $x = 0.21$. The crystalline MMO particles start to undergo segregation into hexagonal and cubic phases upon annealing at 800 °C.

Introduction

The application of mixed metal oxides (MMO) in the production of semiconductor devices,¹ ceramics,² and microelectronics including photoluminescent (PL) devices^{3,4} has triggered much research activity. Stoichiometry and homogeneity of composition are key to the potential applications of such materials.⁵ The size and shape of the MMO particles or microstructure of MMO thin films are important parameters that need to be controlled. For example, the literature shows that, in the synthesis of metal oxide nanoparticles, the formation of a metastable solid solution⁵ or introduction of a second phase⁶ could inhibit the particle growth and enhance the thermal stability with regard to undesired phase transitions.

Many synthetic methods have been described to produce MMO of high and reproducible quality. Mechanical mixing of precursors followed by a firing process to achieve the desired MMO is the traditional method. It starts by ball-milling a mixture of different kinds of pure metal oxides or thermally labile metal salts (e.g., carbonates, acetates, nitrates), and the resulting blend is then subjected to a temperature-controlled heating protocol.⁷ Since it is difficult to control grain growth and segregation phenomena occurring during calcination or sintering, and contaminations may be introduced in the course of blending, it is notoriously troublesome to create high quality

materials. Spray pyrolysis is another method frequently used to synthesize MMO of homogeneous composition at the atomic length scale.⁸ A further method rests on sol–gel chemistry starting from hydrolysis of metal ion containing precursors to produce an intermediate oxy-hydroxyl gel which is then subjected to controlled heating (calcination) to give ceramic powders of desired composition. Sin and Odier⁹ have reported on the synthesis of a series of MMOs of the type $\text{La}_{0.85}\text{Sr}_{0.15}\text{MnO}_3$, $\text{La}_2\text{CuNiO}_6$, and BaZrO_3 in which the EDTA complexes of the metal ions were stabilized in a polyacrylamide gel prepared in situ. The pyrolysis of the dry gel containing the EDTA metal complex at temperatures above 700 °C gave the desired MMO. This is a variation of the Pechini method,¹⁰ which has been widely used in the past. We note for instance the work of Kakihana et al.¹¹ on the synthesis of the perovskite PbTiO_3 using citric acid as both the complexant and reagent to form a water-compatible polyester with ethylene glycol in situ. The gel containing the metal/citric acid complex was then used as a precursor in the calcination. We would like to note an earlier publication by Marcilly and co-workers in which this type of procedure is described in general terms.¹² In all of these cases, the polymer acts as a thermolabile builder to hold the heterogeneous mixture of precursors together.

Hydrothermal synthesis is an approach in which nucleation and growth of the desired MMO particles take place in water or another liquid medium at relatively low temperature and under ambient conditions. Solvent at hydrothermal conditions

- (1) Emons, T. T.; Li, J.; Nazar, L. F. *J. Am. Chem. Soc.* **2002**, *124*, 8516.
- (2) Limthongkul, P.; Wang, H.; Chiang, Y.-M. *Chem. Mater.* **2001**, *13*, 2397.
- (3) Beecroft, L. L.; Ober, C. K. *Adv. Mater.* **1995**, *7*, 1009.
- (4) Taden, A.; Antonietti, M.; Heilig, A.; Landfester, K. *Chem. Mater.* **2004**, *16*, 5081.
- (5) Leite, E. R.; Maciel, A. P.; Weber, I. T.; Lisboa-Filho, P. N.; Longo, E.; Paiva-Santos, C. O.; Andrade, A. V. C.; Pakoschimas, C. A.; Maniette, Y.; Shreiner, W. H. *Adv. Mater.* **2002**, *14*, 905.
- (6) Wu, N.-L.; Wang, S.-Y.; Rusakova, I. A. *Science* **1999**, *285*, 1375.
- (7) Ishii, T.; Furuichi, R.; Nagasawa, T.; Yokoyama, K. *J. Therm. Anal.* **1980**, *19*, 467.

- (8) Marchal, J.; John, T.; Baranwal, R.; Hinklin, T.; Laine, R. M. *Chem. Mater.* **2004**, *16*, 822.
- (9) Sin, A.; Odier, P. *Adv. Mater.* **2000**, *12*, 649.
- (10) Pechini, M. P. U.S. Patent 3,330,697, 1967.
- (11) Kakihana, M.; Okubo, T.; Arima, M.; Uchiyama, O.; Yashima, M.; Yoshimura, M. *Chem. Mater.* **1997**, *9*, 451.
- (12) Marcilly, C.; Courty, P.; Delmon, B. *J. Am. Ceram. Soc.* **1970**, *53*, 56.

provides a mass transport path promoting phase transformation kinetics. $\text{PbZr}_{0.7}\text{Ti}_{0.3}\text{O}_3$ ¹³ and BaTiO_3 ^{14,15} have been obtained using such a method.

Here, we would like to report on a process that differs in important details from previous methods used to prepare MMO powders with controlled composition. The method starts with the preparation of a defined polymer/metal salt complex that is water-soluble and can be purified by repeated precipitation/redissolution cycles and/or dialysis. Such soluble complexes can be prepared to contain two or more different metal ions. The metal ion density which refers to the ratio between the ionogenic sites fixed to the polymer backbone and the number of metal ions per chain can be changed by dilution with nonmetallic counterions. The purified complex in dry form is calcined at relatively low temperature to give nanosized crystals of the MMO provided that sintering can be avoided. The polymer/metal salt solution can also be processed by spin coating, drop casting, or a similar procedure to obtain polymer precursor films. The composition of the precursor polymer defines the stoichiometry of the MMO in cases in which a phase segregation into MMOs of different structure and composition does not occur during calcination.

The method is specifically suited to prepare MMO particles useful as components of polymer/MMO blends. In the following section we use the preparation of zinc/magnesium oxide ($\text{Zn}_{1-x}\text{Mg}_x\text{O}$) as an example but would like to point to our earlier work on the synthesis of submicrometer-sized electrochemically active LiCoO_2 which followed a similar protocol.¹⁶

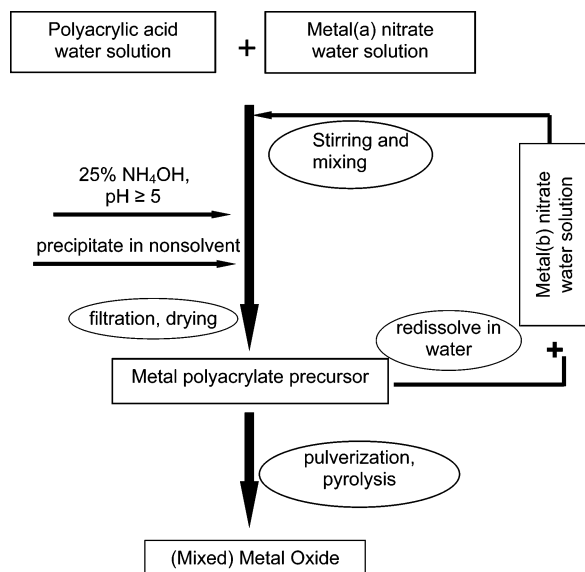
Experimental Details

For a zinc-rich sample ($x < 0.5$), typically, 1.036 g of poly(acrylic acid) (prepared from 50% aqueous solution by freeze drying) ($M_n = 5000$) and 0.428 g of $\text{Zn}(\text{NO}_3)_2 \cdot 6\text{H}_2\text{O}$ were dissolved in 110 mL of water. Nitrogen was bubbled through the solution to remove carbon dioxide for 10 min. Ammonium hydroxide (25 wt %) was added dropwise to adjust the pH to the desired value between 5 and 10. The reaction mixture was concentrated to about 20 mL by vacuum distillation. The residual viscous liquid was dropped into 120 mL of acetone. A colorless precipitate was formed and collected by centrifugation. It was washed with acetone and dried at 40 °C in vacuo. This material (0.5 g) was redissolved in 50 mL of water. A solution of 0.144 g of $\text{Mg}(\text{NO}_3)_2 \cdot 6\text{H}_2\text{O}$ in 15 mL of water was added. The pH was adjusted to 7 with ammonia. The mixed solution was concentrated to 20 mL in vacuo and then poured dropwise into 100 mL of acetone. The precursor material was collected by centrifugation, washed with acetone, and dried in vacuo. It was milled into a fine powder and then calcined in a temperature-controlled oven under air flow at a heating rate of 5 °C min^{-1} to 550 °C. The sample was isothermally annealed for 1 h at this temperature.

For the Mg-rich samples ($x > 0.5$), the analogous magnesium polyacrylate complex was first prepared, and then zinc was incorporated as described above.

The composition with regard to Zn and Mg in the precursors and the MMOs was determined by atomic absorption spectroscopy (AAS) using a Perkin-Elmer 5100 ZL spectrometer. The zinc/magnesium polyacrylate complex was dissolved in water, while the $\text{Zn}_{1-x}\text{Mg}_x\text{O}$ samples were dissolved in concentrated HCl. pH was measured with a Pt/KCl glass electrode attached to a pH meter (Schott CG 843 set).

Scheme 1. Synthesis of MMO Powders by Pyrolysis of Mixed Metal Polyacrylates



The optimal temperature for calcination was worked out by thermogravimetric analysis (TGA), using a Mettler Toledo TGA/SDTA 851e instrument. Powder X-ray diffraction patterns were recorded on a Seifert 3000 TT Bragg-Brentano diffractometer using $\text{Cu K}\alpha$ radiation with $\lambda = 0.15406$ nm, operating at 40 kV and 30 mA with a 0.03° step size in the range of $5^\circ \leq 2\theta \leq 80^\circ$. TEM images were obtained by Tecnai F20 microscope operating at 200 kV. An energy-dispersive X-ray (EDX) spectrometer was coupled to the TEM for composition determination. PL measurements were obtained at room temperature from a Spex Fluorolog spectrometer.

Results and Discussion

The polymer-based process of synthesis of MMO is outlined in Scheme 1. It starts by codissolving relatively low molecular weight poly(acrylic acid) ($M_n = 5000$ g mol^{-1}) and a zinc salt (e.g., $\text{Zn}(\text{NO}_3)_2$) in water followed by adjusting the pH to values larger than 5. A 4-fold molar excess of carboxylic groups vis. zinc is chosen. The clear solution is poured into acetone, whereupon the zinc polyacrylate complex precipitates out. It is redissolved in water; the desired amount of magnesium nitrate is added, and the zinc/magnesium polyacrylate complex is obtained by precipitation from acetone. The precipitation serves to purify the precursor by removing the ionic impurities and other species in the reaction mixture. After drying in vacuo, the solid polymer metal ion complex appears as a colorless, completely amorphous powder as indicated by X-ray diffraction as well as TEM results. It is worthwhile mentioning that the polyacrylate zinc magnesium complex prepared this way is completely soluble in water with a viscosity behavior that conforms to ordinary polyelectrolytes.^{17,18}

The dry precursor powder is converted into $\text{Zn}_{1-x}\text{Mg}_x\text{O}$ by heating it in oven under air flow at a heating rate of 5 °C/min to 550 °C and then keeping it at that temperature for 1 h. The resulting colorless powder is composed of nanosized crystals,

- (13) Oledzka, M.; Lencka, M. M.; Pinceloup, P.; Mikulka-Bolen, K.; McCandlish, L. E.; Riman, R. E. *Chem. Mater.* **2003**, *15*, 1090.
 (14) Oledzka, M.; Brese, N. E.; Riman, R. E. *Chem. Mater.* **1999**, *11*, 1931.
 (15) Grohe, B.; Miehle, G.; Wegner, G. *J. Mater. Res.* **2001**, *16*, 1901.
 (16) Lan, L.; Meyer, W.; Wegner, G.; Wohlfahrt-Mehrens, M. *Adv. Mater.* **2005**, *17*, 984.

- (17) Kulicke, W.-M.; Clasen, C. *Viscosimetry of Polymers and Polyelectrolytes*; Springer-Verlag: Berlin, 2004; p 61.
 (18) Förster, S.; Schmidt, M. *Adv. Polym. Sci.* **1995**, *120*, 51.
 (19) The software can be downloaded free of charge via www.ccp14.ac.uk/ccp/web-mirrors/lmgp-laugier-bochu/.
 (20) The data was obtained from the Joint Committee on Powder Diffraction Standards (JCPDS) card 36-1451, International Center for Diffraction Data.

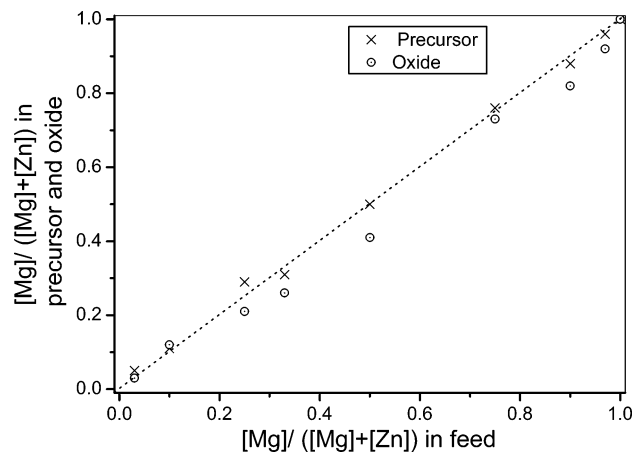


Figure 1. Ratio of Mg content to whole metal content in feed versus that determined in the polymer precursor (x) and mixed metal oxide (O) by means of AAS.

and it has a composition (i.e., $x = [\text{Mg}]/([\text{Mg}] + [\text{Zn}])$) predefined by the magnesium content to the overall metal content ratio in the polymer precursor as shown in Figure 1. The magnesium content in the polymer precursor reflects this ratio in the feed. Here a slight depletion of magnesium in the range of $x = 0.2\text{--}0.6$ takes place in the mixed metal oxides samples.

Figure 2a shows the X-ray diffraction patterns of the oxide products covering the whole composition range. The patterns of the pure ZnO are indexed according to the known hexagonal phase (zincite), and that of MgO is indexed according to its cubic phase (periclase). Clear indications for segregation into a hexagonal and a cubic phase are found for samples having magnesium content between $0.26 \leq x \leq 0.73$. Samples of $x = 0.21$ and 0.26 showed a very weak (200) reflection of the MgO phase, indicating that the majority of the material was in the form of zincite. At composition of $\text{Zn}_{0.88}\text{Mg}_{0.12}\text{O}$, the hexagonal phase was the only one seen. The appearance of reflections in the powder patterns belonging to two different phases indicates that particles that differ in phase structure and elemental composition have been formed in a particular range of overall composition at the temperature and time interval of the calcination. Figure 2b shows the dependence of the lattice parameter of the hexagonal phase depending on the overall Mg content. While the unit cell clearly shrinks along the c -axis from the value of the pure hexagonal ZnO phase with increasing magnesium content, this is not true for the a -axis parameter. These results are roughly in agreement with the data obtained from epitaxially grown films on sapphire by a laser deposition method,²¹ although in detail there are significant differences. In particular, the onset of MgO segregation from the zincite phase occurs already at smaller values in our samples and the dependence of the c -parameter on composition is stronger. These differences may be a consequence of the different preparation methods and the adhesion to the substrate in the laser deposited films. We also would like to mention the work of Shan et al.,²² who reported a linear decrease of the lattice constants with increasing magnesium content between $0 \leq x \leq$

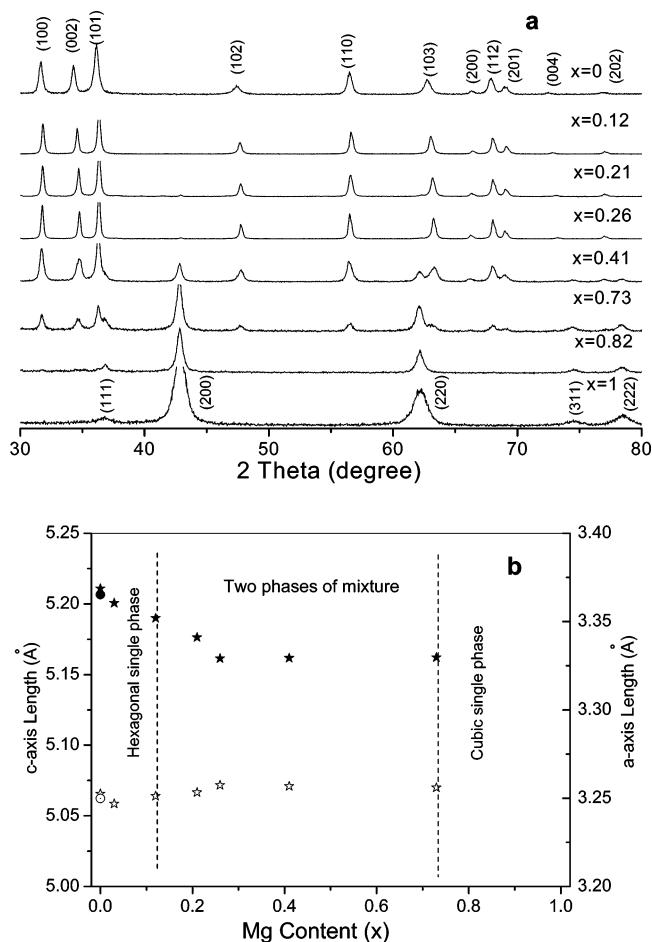


Figure 2. (a) X-ray diffraction patterns of $\text{Zn}_{1-x}\text{Mg}_x\text{O}$ ($0 \leq x \leq 1$). Note that at $x = 0.21$ the (200) peak of cubic phase begins to appear. (b) Cell parameter c (filled star) and a (open star) as a function of the Mg content x . The data were refined by CELREF.¹⁹ Filled and open circles indicate the standard values of ZnO cell parameters.²⁰ The two dashed lines mark the phase boundary.

0.05 with the same trend seen by us. These authors used laser deposition as well but on glass as the substrate. Their value quoted at $x = 0.05$ is within the error margin of our findings. However, we do not see a similar change in the a -axis parameter. To this point our result is in agreement with that of Ohtomo et al.²¹

The data reported in Figure 3 give evidence that our samples consist of nanometer-sized crystals of homogeneous composition. Figure 3a shows a TEM image of a large number of crystals having the overall composition $\text{Zn}_{0.88}\text{Mg}_{0.12}\text{O}$. The inset shows the electron diffraction pattern of this particle collection which is consistent with the pattern of ZnO. Figure 3b presents a high-resolution (HRTEM) image of a single particle of this sample showing (100) and (012) lattice fringes and crystalline order on the length scale of the size of the crystals. Actually, crystal defects such as dislocations and stacking faults are also found in some other TEM images. Figure 3c gives results of an EDX spectroscopy line scan analyzing a particle for its composition. The similarity of the profile of Mg and Zn composition proves that both elements are homogeneously distributed over the whole particle. In other words, magnesium ions are able to occupy places of zinc ions in the zincite lattice forming a solid solution. We note that the phase diagram of the system ZnO/MgO predicts the formation of a solid

(21) Ohtomo, A.; Kawasaki, M.; Koida, T.; Masubuchi, K.; Koinuma, H.; Sakurai, Y.; Yoshida, Y.; Yasuda, T.; Segawa, Y. *Appl. Phys. Lett.* **1998**, *72*, 2466.

(22) Shan, F. K.; Kim, B. I.; Liu, G. X.; Liu, Z. F.; Sohn, J. Y.; Lee, W. J.; Shin, B. C.; Yu, Y. S. *J. Appl. Phys.* **2004**, *95*, 4772.

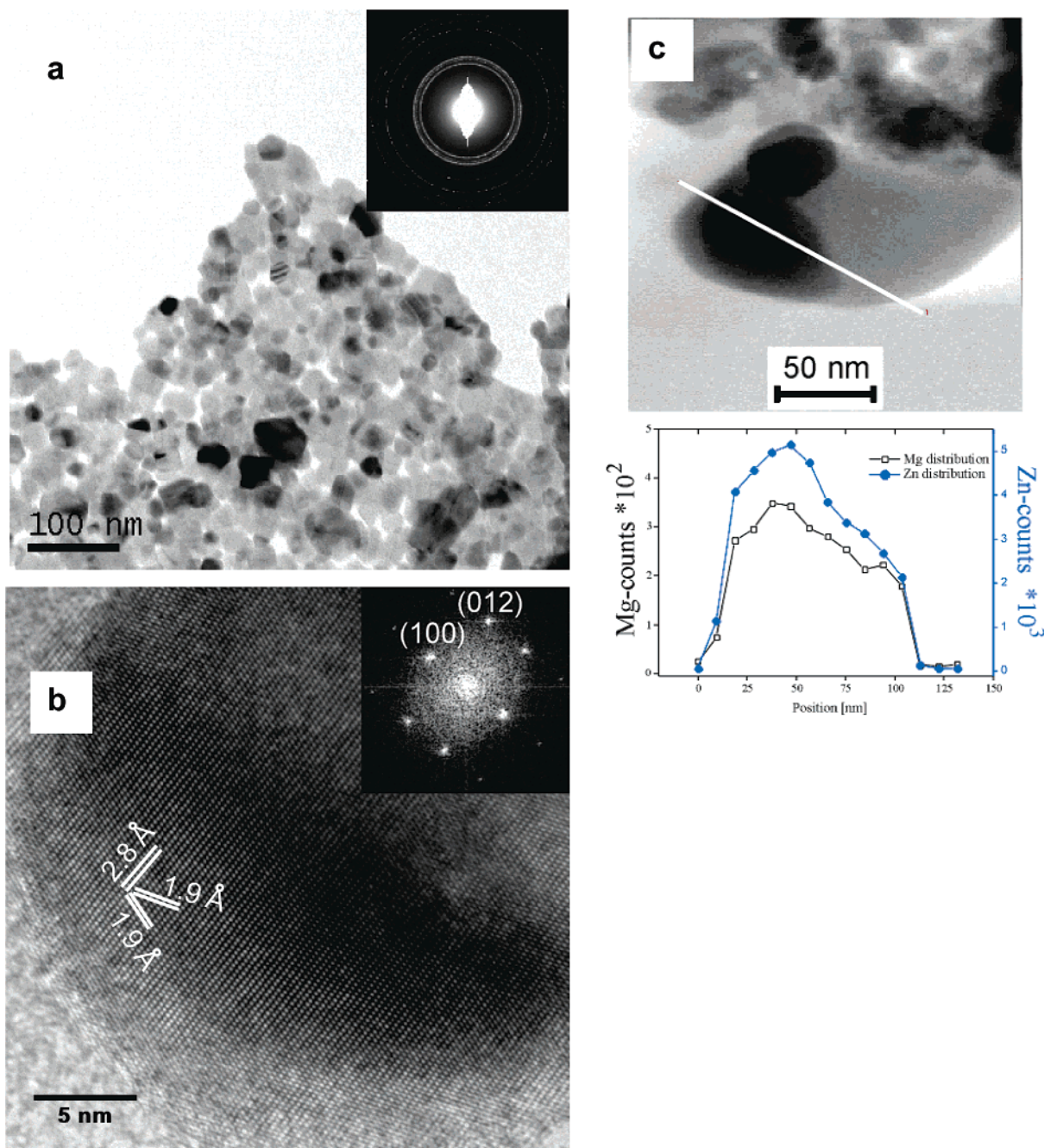


Figure 3. (a) TEM image showing the morphology of $\text{Zn}_{0.88}\text{Mg}_{0.12}\text{O}$ nanoparticles. The inset is the electron diffraction pattern. The spotty nature of the pattern indicates that the nanocrystallites are three-dimensionally randomly oriented. (b) HRTEM image of one particle of the same sample. The inset is the corresponding fast Fourier transform of the image. (c) EDX results of Zn and Mg with a line scan as denoted by the line.

solution of both components near the ZnO boundary.²³ However, the amount of MgO in solid solution in the zincite structure is only about 2 wt % (corresponding to a molar fraction of 0.04) at equilibrium conditions (1600 °C). In our case, the phase formation occurs far from equilibrium and from an amorphous precursor at 550 °C. Hence, our nanometer-sized crystals are metastable insofar as their composition is not the equilibrium composition. In fact, short annealing of the solid solution-type crystals in the zincite phase at a temperature of 800 °C for 2 h shows the beginning of periclase phase segregation from the zincite phase. The intensity of the X-ray diffraction peak for MgO (200) is about 0.6% of that of ZnO (002). The weakly

agglomerated particles depicted in Figure 3 can be separated by a short treatment with ethanolic solution of tetrabutylammonium phosphate and applying ultrasonication. Mostly individual crystals are obtained as detected by scanning electron microscopy.

The presence of magnesium on lattice sites of zinc has consequences for the electronic properties. ZnO is a wide band gap semiconductor ($E_g = 3.34$ eV), while MgO has a band gap as large as 7.5 eV.²⁴ Incorporating Mg atoms on Zn lattice sites will increase the band gap of ZnO. This is called band gap engineering, and it will change the electrical and optical

(23) Segnit, E. R.; Holland, A. E. *J. Am. Ceram. Soc.* **1965**, *48*, 409.

(24) Chen, J.; Shen, W. Z. *Appl. Phys. Lett.* **2003**, *83*, 2154.

properties of the material.²⁵ In fact, many publications deal with the optical properties of doped ZnO; however, they are mostly for samples obtained in the form of thin film on solid substrate such as quartz, sapphire, and so on.^{21,22,26} The spectral data and particularly data on PL reported in the literature differ considerably. They demonstrate that the preparation method of the films or powders has a strong impact on the optics of the material. ZnO exhibits relatively intense photoluminescence. Generally, two peaks are seen in the PL emission spectrum of pure ZnO. One of these is relatively weak and centered around 3.24 eV. It is associated with the near band edge (NBE) emission. The other one occurs in the visible region of the spectrum. It is frequently recorded with the maximum centered around 2.12 eV, intensity and precise position depending on preparation conditions, purity and thermal history of the sample. The origin of this emission is not totally clear, but it is generally assumed that it originates from oxygen defect levels²⁷ either in the bulk or at the surface of the crystals. In our case, doping of magnesium into the ZnO phase has a strong quenching effect on the high-energy NBE emission while emission in the visible is enhanced. Figure 4a shows the PL excitation spectra of the emission in the visible for our powder samples of $\text{Zn}_{1-x}\text{Mg}_x\text{O}$ for various values of x . Figure 4b shows the corresponding PL emission spectra. The PL excitation spectra were recorded measuring the intensity of the PL emission at the respective maximum for each composition. The excitation spectrum monitors the density of states near the band edge and allows retrieval of the band gap energy from the adsorption edge. The strong dependence of the absorption edge on Mg concentration is evident. This effect had been seen previously and has been discussed in detail for epitaxially grown thin films.^{21,22} Our materials behave similarly, although they are nanosized powders and not monodomain epitaxially grown films.

Another point worth noting is the significant decrease of slope with increasing Mg concentration in the PL excitation spectra near the band edge. This effect is known as alloy broadening, but the excitonic character of the absorption peak remains. The emission in the visible shifts from pure ZnO with maximum at 2.12 eV to 2.32 eV at $x = 0.21$ (when the segregation into MgO and ZnO phase occurs); it then jumps to about 2.8 eV in the MgO phase alloy. The band gap and associated excitation spectral characteristics change nearly linearly with increasing content of Mg in the zinc-rich part of the phase composition as indicated in Figure 4c. Contrary to this, the energy of the PL emission and its shape seem to saturate near a composition of $x = 0.2$. We would like to interpret this phenomenon by the assumption that the PL emission comes from localized defect centers which are relatively weakly affected by the change in the band structure of the material, which in turn responds strongly to the substitutional replacement of zinc by magnesium. A thus far inexplicable phenomenon just for one sample of

- (25) (a) Ourmazd, A.; Hall, R.; Tung, R. T. In *Materials Science Technology*; Cahn, R. W., Haasen, P., Kramer, E. J., Eds.; Wiley-VCH: Weinheim, Germany, 1996; Vol. 4, p 3818. (b) Bailey, R. E.; Nie, S. M. *J. Am. Chem. Soc.* **2003**, *125*, 7100. (c) Kim, S.; Fisher, B.; Eislner, H.-J.; Bawendi, M. *J. Am. Chem. Soc.* **2003**, *125*, 11466.
- (26) (a) Ohtomo, A.; Shiroki, R.; Ohkubo, I.; Koinoma, H.; Kawasaki, M. *Appl. Phys. Lett.* **1999**, *75*, 4088. (b) Sharma, A. K.; Narayan, J.; Muth, J. F.; Teng, C. W.; Jin, C.; Kvit, A.; Kolbas, R. M.; Holland, O. W. *Appl. Phys. Lett.* **1999**, *75*, 3327. (c) Jin, Y.; Zhang, B.; Yang, S.; Wang, Y.; Chen, J.; Zhang, H.; Huang, C.; Cao, C.; Cao, H.; Chang, R. P. H. *Solid State Commun.* **2001**, *119*, 409. (d) Dev, A.; Chakrabarti, S.; Kar, S.; Chaudhuri, S. *J. Nanopart. Res.* **2005**, *7*, 195.
- (27) Vanheusden, K.; Seager, C. H.; Warren, W. L.; Tallant, D. R.; Voigt, J. A. *Appl. Phys. Lett.* **1996**, *68*, 403.

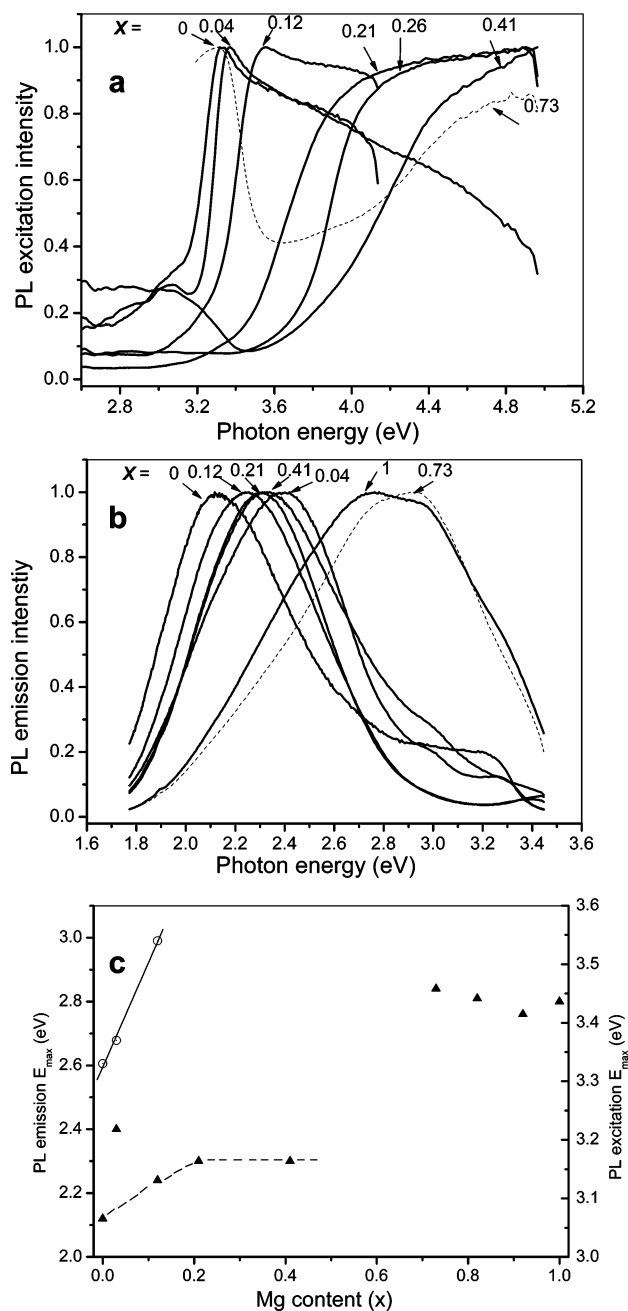


Figure 4. (a) PL excitation spectra of samples of $\text{Zn}_{1-x}\text{Mg}_x\text{O}$ with different x . (b) PL emission spectra of $\text{Zn}_{1-x}\text{Mg}_x\text{O}$ samples excited at 325 nm. (c) Maxima of PL emission (\blacktriangle) and excitation (\circ) E_{max} depending on x ; the broken line through the data points of PL emission is a guide to the eye.

composition $\text{Zn}_{0.96}\text{Mg}_{0.04}\text{O}$ is observed. This sample showed the maximum of PL emission at 2.4 eV, which is much blue-shifted from what could be expected from the data of the other compositions. At present, we must leave it to further experimentation to clarify the origin of this behavior. We would also like to note the observation that the NBE emission is quenched on alloying while the emission in the visible is enhanced, which indicates that the number of the defect sites associated with the emission is strongly enhanced.

Conclusion

In summary, we have demonstrated that the calcination of a polymer/metal salt complex which can be purified and processed following established methods of polymer chemistry is useful

to prepare nanosized crystals of a typical MMO. The preparation of $\text{Zn}_{1-x}\text{Mg}_x\text{O}$ by controlled pyrolysis of a zinc/magnesium polyacrylate complex is used as an example. The particles of typically 20–50 nm in diameter are single crystals and are metastable alloys of the ZnO/MgO systems in a particular range of composition. Effects of band gap engineering on the optical band gap are seen and are in general agreement with expectation. The photoluminescence in the visible is enhanced while the high-energy emission in the UV region is suppressed by incorporation of magnesium ions on zinc ion lattice sites. This points toward the usefulness of our approach to create photo emissive materials with enhanced sensitivity. However, significant differences in the emission profiles are seen in our materials

compared to the reported data from literature indicating the impact of processing conditions on the electronic properties.

We believe that this method has a wide scope of application for the preparation of powders of mixed metal oxide alloys of metastable type from a polymer metal ion complex as the precursor which is converted to the MMO at relatively low temperature where sintering is not yet prevailing.

Acknowledgment. G.L. gratefully acknowledges support by a scholarship from the Max Planck Society. We acknowledge assistance in obtaining useful data by B. Mathiasch (AAS data) and H. Menges (PL data).

JA0638096